

Gd³⁺-functionalized near-infrared quantum dots for *in vivo* dual modal (fluorescence/magnetic resonance) imaging†

Takashi Jin,^{*ab} Yoshichika Yoshioka,^{ab} Fumihiko Fujii,^a Yutaka Komai,^a Junji Seki^{ac} and Akitoshi Seiyama^{bd}

Received (in Cambridge, UK) 17th July 2008, Accepted 5th September 2008

First published as an Advance Article on the web 6th October 2008

DOI: 10.1039/b812302k

Gd³⁺-functionalized near-infrared emitting quantum dots were synthesized as a dual modal contrast agent for *in vivo* fluorescence imaging and magnetic resonance imaging.

Semiconductor quantum dots (QDs) are a new class of fluorescent materials for use in biolabeling, biosensing, and bioimaging.^{1,2} Compared with traditional organic fluorophores and fluorescent proteins, QDs have unique optical properties such as size-dependent emission, high brightness, narrow emission and broad absorption spectra, and high resistance to photobleaching.^{1,2} For the past decade, synthetic methods for the preparation of visible-emitting QDs (*e.g.* CdS, CdSe, CdTe) have been developed.^{3–5} Visible-emitting QDs, however, have a disadvantage in the application to *in vivo* fluorescence imaging. Visible light (400–650 nm) is strongly absorbed by intrinsic chromophores such as hemoglobin.^{6–8} The light that shows lowest absorption and scattering in living tissues is near-infrared (NIR) light ranging from 700 to 900 nm.⁶

The major advantage of NIR-fluorescence imaging is the capability of visualizing target objects (*e.g.* tumors and vasculatures) in deeper tissues (0.5 mm–cm) with a low background signal.⁶ However, the spatial resolution of NIR-fluorescence imaging is not enough to show a 3-dimensional object's location with an anatomical resolution. Magnetic resonance imaging (MRI) is one of the imaging techniques used for obtaining 3-dimensional information. In MRI, paramagnetic ions such as Gd³⁺ and Fe³⁺ are often used to improve the contrast of MR images. Here, we report Gd³⁺-functionalized NIR-emitting QDs that can be used for both *in vivo* NIR-fluorescence imaging and MRI. The Gd³⁺-functionalized water-soluble NIR-QDs were prepared based on hydrophobic CdSeTe/CdS (core-shell) QDs.

Fig. 1 shows a synthetic procedure for preparing Gd³⁺-functionalized NIR-QDs. We first synthesized hydrophobic NIR-QDs (CdSeTe/CdS) by a modified method based

on the synthetic procedure previously reported.^{9,10} In the hydrophobic CdSeTe/CdS QDs, the surface of the QDs is capped with trioctylphosphine (TOP), trioctylphosphine oxide (TOPO), and hexadecylamine (HDA).^{9,10} Hence, the QDs are highly hydrophobic and not soluble in water. Bailly *et al.* first reported a water-solubilization method for CdSeTe/CdS QDs using mercaptoacetic acid as a surface coating agent.¹⁰ Although the resulting QDs retain the fluorescence intensity of the uncoated QDs after the surface coating, the coated QDs precipitate out of solution after 2–3 weeks.¹⁰ Recently, Jiang *et al.* reported water-soluble CdSeTe/CdS QDs that are coated with mercaptoundecanoic acids.¹¹ In this work, we used a natural thiol compound, glutathione (GSH, reduced form) as a surface coating agent. GSH is a tripeptide (γ -L-glutamyl-L-cysteinylglycine) that exists in most tissues and can be used to detoxify Cd²⁺ ions due to its chelating capability.¹² When the CdSeTe/CdS QDs are coated with GSH, the resulting QDs retain *ca.* 60% of the fluorescence intensity. The colloidal stability of the GSH-coated CdSeTe/CdS QDs is much better than that of mercaptoacetic acid-coated CdSeTe/CdS QDs, and stable (> 1 month) in phosphate buffered saline (PBS, pH = 7.4). To add the MRI contrast ability to the GSH-QDs, we functionalized the surface of the QDs with Gd³⁺-DOTA (1,4,7,10-tetraazacyclododecane-1,4,7,10-tetraacetic acid) complexes (ESI†).

To confirm the binding of Gd³⁺-DOTA complexes to the surface of QDs, we measured the size of QDs before and after

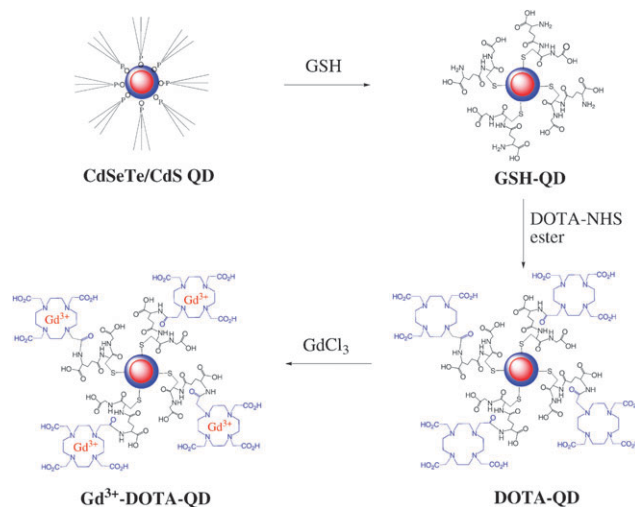


Fig. 1 Schematic representation for the preparation of Gd³⁺-DOTA functionalized CdSeTe/CdS QDs with glutathione (GSH) coating.

^a WPI Immunology Frontier Research Center, Osaka University, Suita, Osaka 565-0871, Japan. E-mail: jin@fbs.osaka-u.ac.jp; Fax: +81-6-6879-4426; Tel: +81-6-6879-4427

^b Graduate School of Frontier Biosciences, High Performance Bioimaging Facility, Suita, Osaka University, Osaka 565-0871, Japan

^c National Cardiovascular Center Research Institute, Suita, Osaka 565-8561, Japan

^d Graduate School of Medicine, Kyoto University, Kyoto 606-8507, Japan

† Electronic supplementary information (ESI) available: Details for synthesis and characterization data for Gd-DOTA-QDs. See DOI: 10.1039/b812302k

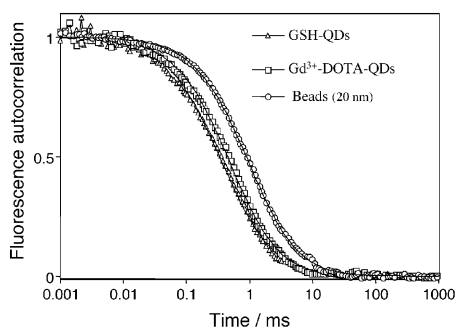


Fig. 2 Fluorescence autocorrelation curves for GSH-QDs, Gd^{3+} -DOTA-QDs and fluorescent beads in PBS buffer (pH = 7.4). The autocorrelation curves are fitted by using a one-component diffusion model (solid lines).

the conjugation reaction using fluorescence correlation spectroscopy (FCS, see ESI†),^{13–15} FCS uses the fluctuation of fluorescence intensity in a tiny excitation volume to determine the diffusion times of fluorescent molecules. Fig. 2 shows fluorescence autocorrelation curves for GSH-QDs and Gd^{3+} -DOTA-QDs in PBS. For comparison, an autocorrelation curve for fluorescent beads (20 nm in diameter, Molecular Probe, Inc.) is also shown. All fluorescence autocorrelation curves can be fitted to a one-component diffusion model, and the diffusion times are determined to be 0.35 ± 0.02 ms, 0.51 ± 0.01 ms, and 0.99 ± 0.05 ms for GSH-QDs, Gd^{3+} -DOTA-QDs, and the reference beads, respectively. Assuming a spherical body of QDs, hydrodynamic diameters are calculated to be 7.0 ± 0.4 nm and 10 ± 0.2 nm for GSH-QDs and Gd^{3+} -DOTA-QDs, respectively (ESI†). This result shows that the hydrodynamic diameter of Gd^{3+} -DOTA-QDs increases by a factor of 30% as a result of the binding of Gd^{3+} -DOTA¹⁶ to the surface of GSH-QDs.

In NIR-fluorescence imaging *in vivo*, the brightness of fluorescent probes is crucial for obtaining clear images with a high signal to noise ratio. We compared the absorption and fluorescence spectra of Gd^{3+} -DOTA-QDs with those of indocyanine green (ICG) which is a widely used NIR-fluorescent dye for *in vivo* imaging¹⁷ (Fig. 3). The absorption of the Gd^{3+} -DOTA-QDs shows a broad spectrum, indicating that the QDs can be excited by NIR-light ($< ca.$ 800 nm) as well as visible light (400–700 nm). In the case of ICG, the excitation wavelengths are limited to the region of *ca.* 600–800 nm. When Gd^{3+} -DOTA-QDs (in PBS) and ICG (in DMSO) are excited at 695 nm where the absorbance is set to be the same value, the

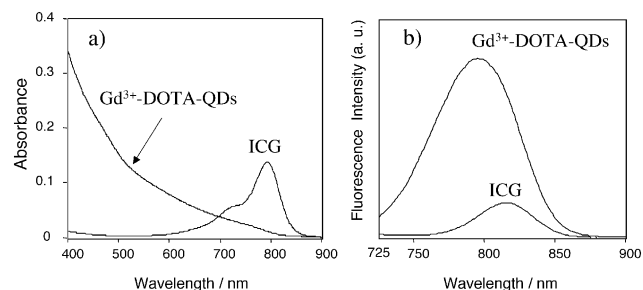


Fig. 3 (a) Absorption and (b) fluorescence spectra of Gd^{3+} -DOTA-QDs in PBS and ICG in DMSO. The fluorescence spectra were measured at an excitation wavelength of 695 nm, where the absorbance was set to be the same value of 0.035 for both solutions.

fluorescence intensity of the Gd^{3+} -DOTA-QDs is 7 times higher than that of ICG.¹⁸

To check the ability of the Gd^{3+} -DOTA-QDs to act as a MRI contrast agent, we measured T_1 weighted MR images. Fig. 4(a) shows a T_1 weighted image for saline, aqueous solutions of GSH-QDs (10 μM) and Gd^{3+} -DOTA-QDs (10 μM). The T_1 weighted image of GSH-QDs shows a similar contrast with that of saline, used as a reference. In contrast, the T_1 weighted image of the Gd^{3+} -DOTA-QDs is much brighter than that of saline and GSH-QDs. Fig 4(b) shows the effects of Gd^{3+} -DOTA-QD concentration on the T_1 weighted image. Using a saturation recovery method, the values of T_1 were determined and the R_1 relaxivity for Gd^{3+} -DOTA-QDs was calculated to be $365 \text{ mM}^{-1} \text{ s}^{-1}$ (ESI†). We also measured T_2 weighted MR images and the R_2 relaxivity for Gd^{3+} -DOTA-QDs was determined to be $6779 \text{ mM}^{-1} \text{ s}^{-1}$ (ESI†).

To test the utility of the Gd^{3+} -DOTA-QDs as a dual modal contrast agent for *in vivo* imaging, we performed NIR-fluorescence imaging and MRI for a mouse, where a phantom (a polyethylene tube with 1.5 mm diameter) containing 5 ml of Gd^{3+} -DOTA-QDs (10 μM) was embedded into a mouse abdomen (Fig. 5).[†] NIR-fluorescence images were obtained by irradiation of a 785 nm diode laser with a 845 nm band-pass filter. The phantom strongly emits NIR-fluorescence from the inside of the mouse abdomen, and the location of the phantom can be estimated at two-dimensional level (Fig. 5a). However, the NIR-fluorescence image does not show 3-dimensional location of the phantom with an anatomical resolution. The precise location of the phantom in the mouse can be determined from the T_1 weighted MR image (Fig. 5b). The MR image of the phantom containing Gd^{3+} -DOTA-QDs is brighter than that of surrounding tissues in the mouse. The imaging data using a phantom indicate that Gd^{3+} -DOTA-QDs are useful as a dualmodal contrast agent for NIR-fluorescence imaging and MRI. Thus, the combination of NIR-fluorescence and MRI images would enable facile identification of the location of target cells and/or tissues labeled with the Gd^{3+} -DOTA-QDs.

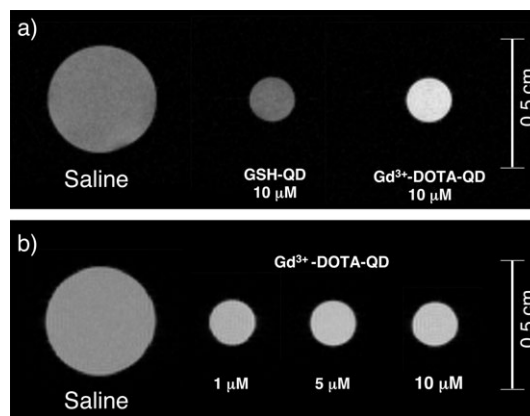


Fig. 4 (a) T_1 weighted MR images for saline, GSH-QDs and Gd^{3+} -DOTA-QDs in PBS. (b) Concentration dependence of Gd^{3+} -DOTA-QDs on the T_1 weighted MR image. Saline (0.9% NaCl aqueous solution) is used as a reference.

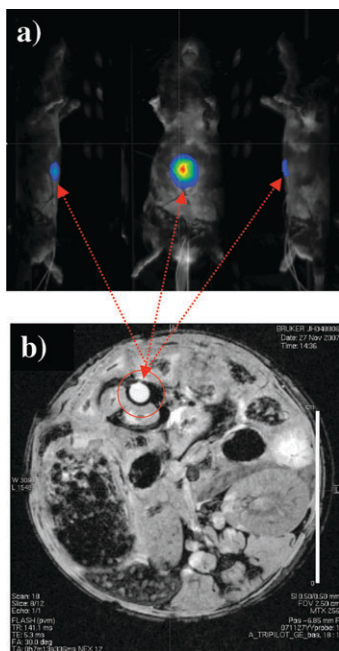


Fig. 5 (a) A NIR-fluorescence image and (b) a T_1 weighted MR axial image for a mouse. A phantom containing $10\ \mu\text{M}$ of Gd^{3+} -DOTA-QDs is embedded into the mouse abdomen. The arrow heads on the red broken lines represent the location of the phantom being visualized by fluorescence imaging and MRI. The white bar in the MRI image corresponds to 1 cm in length.

In conclusion, we have presented a synthetic method for the NIR-emitting Gd^{3+} -DOTA-QDs and their utility as a dual modal contrast agent for *in vivo* fluorescence imaging and MRI. So far, several reports regarding dual modal QDs for bioimaging have appeared.^{19–26} However, most of the reports are limited to the visible light-emitting QDs with a MRI contrast ability. This is the first report of dual modal QDs that can be used for NIR-fluorescence imaging and MRI *in vivo*. We intend to apply dual modal Gd^{3+} -DOTA-QDs to the visualization of cancerous tumors and lymph nodes.

This work was partly supported by the Ministry of Education, Science, Sport and Culture of Japan (Grant-in-Aid for Scientific Research, No. 19550157), and by CREST of Japan Science and Technology Agency (JST). One (T. J.) of the authors thanks Prof. T. Yagi and Dr R. Kaneko for their helpful discussions. The authors thank Dr I. Oda and T. Ohyagi for use of a prototype *in vivo* imaging apparatus (Shimadzu Co., Japan).

Notes and references

† All experiments were performed in compliance with the National Institutes of Health Guidelines for the Care and Use of Laboratory Animals, and were approved by the Osaka University Animal Care and Use Committee.

- (a) M. Bruchez Jr, M. Moronne, P. Gin, S. Weiss and A. P. Alivisatos, *Science*, 1998, **281**, 2013–2016; (b) W. C. W. Chan and S. Nie, *Science*, 1998, **281**, 2016–2018.
- (a) X. Gao, L. Yang, J. A. Petros, F. F. Marshall, J. W. Simons and S. Nie, *Curr. Opin. Biotechnol.*, 2005, **16**, 63–72; (b) X. Michalet, F. F. Pinaud, L. A. Bentolila, J. M. Tsay, S. Doose, J. J. Li, G. Sundaresan, A. M. Wu, S. S. Gambhir and S. Weiss, *Science*, 2005, **307**, 538–544; (c) I. L. Medintz, T. Uyeda, E. R. Goldman and H. Mattoussi, *Nat. Mater.*, 2005, **4**, 435–446.
- M. A. Hines and P. Guyot-Sionnest, *J. Phys. Chem.*, 1996, **100**, 468–471.
- B. O. Dabbousi, J. Rodriguez-Viejo, F. V. Mikulec, J. R. Heine, J. H. Mattoussi, R. Ober, K. F. Jensen and M. G. Bawendi, *J. Phys. Chem. B*, 1997, **101**, 9463–9475.
- L. Qu and X. Peng, *J. Am. Chem. Soc.*, 2002, **124**, 2049–2055.
- (a) R. A. Weissleder, *Nat. Biotechnol.*, 2001, **19**, 316–317; (b) W. M. Leevy, T. N. Lambert, J. R. Johnson, J. Morris and B. D. Smith, *Chem. Commun.*, 2008, 2331–2333.
- H. Liu, B. Beauvoit, M. Kimura and B. Chance, *J. Biomed. Opt.*, 1996, **1**, 200–211.
- Y. T. Lim, S. Kim, A. Nakayama, N. E. Stott, M. G. Bawendi and J. V. Frangioni, *Mol. Imaging*, 2003, **2**, 50–64.
- R. E. Baily and S. Nie, *J. Am. Chem. Soc.*, 2003, **125**, 7100–7106.
- R. E. Baily, J. B. Strausburg and S. Nie, *J. Nanosci. Nanotechnol.*, 2004, **4**, 569–574.
- W. Jiang, A. Singhal, J. Zheng, C. Wang and W. C. W. Chan, *Chem. Mater.*, 2006, **18**, 4845–4854.
- R. K. Singhal, M. E. Anderson and A. Meister, *FASEB J.*, 1987, **1**, 220–223.
- T. Jin, F. Fujii, H. Sakata, M. Tamura and M. Kinjo, *Chem. Commun.*, 2005, 2829–2831.
- T. Jin, F. Fujii, E. Yamada, Y. Nodasaka and M. Kinjo, *J. Am. Chem. Soc.*, 2006, **128**, 9288–9289.
- R. F. Heuff, J. L. Swift and D. T. Cramb, *Phys. Chem. Chem. Phys.*, 2007, **9**, 1870–1880.
- The average number of Gd^{3+} -DOTA complexes per QD particle was determined to be 77 ± 18 . See ESI†.
- J. V. Frangioni, *Curr. Opin. Chem. Biol.*, 2003, **7**, 626–634.
- The quantum yields of ICG are 0.3% in water, 1.2% in blood, and 12% in DMSO at an excitation wavelength of 765 nm. See R. C. Benson and H. A. Kues, *Phys. Med. Biol.*, 1978, **23**, 159–163.
- (a) H. Gu, R. Zheng, X. Zhang and B. Xu, *J. Am. Chem. Soc.*, 2004, **126**, 5664–5665; (b) H. Gu, R. Zheng, H. Liu, X. Zhang and B. Xu, *Small*, 2005, **4**, 402–406.
- (a) W. B. Tan and Y. Zhang, *Adv. Mater.*, 2005, **17**, 2375–2380; (b) W. B. Tan and Y. Zhang, *J. Nanosci. Nanobiotechnol.*, 2007, **7**, 2389–2393.
- (a) S. Santra, H. Yang, P. H. Holloway, J. T. Stanley and R. A. Mericle, *J. Am. Chem. Soc.*, 2005, **127**, 1656–1657; (b) H. Yang, S. Santra, G. A. Walter and P. H. Holloway, *Adv. Mater.*, 2006, **18**, 2890–2894.
- W. J. M. Mulder, R. Koole, R. J. Brandwijk, G. Storm, P. T. K. Chin, G. J. Strijkers, C. M. Donega, K. Nicolay and A. W. Griffioen, *Nano Lett.*, 2006, **1**, 1–6.
- (a) G. A. F. van Tilborg, W. J. M. Mulder, P. T. K. Chin, G. Storm, C. P. Reutelingsperger, K. Nicolay and G. J. Strijkers, *Bioconjugate Chem.*, 2006, **17**, 865–868; (b) L. Prinzen, R. J. H. M. Misesus, A. Dirksen, T. M. Hackeng, N. Deckers, N. J. Bitsch, R. T. A. Megens, K. Douma, J. W. Heemskerk, M. E. Kooi, P. M. Frederik, D. W. Slaaf, M. A. M. J. van Zandvoort and C. P. M. Reutelingsperger, *Nano Lett.*, 2007, **7**, 93–100.
- S. Wang, B. R. Jarrett, S. M. Kauzlarich and A. Y. Louie, *J. Am. Chem. Soc.*, 2007, **129**, 3848–3856.
- S. T. Selevan, P. K. Patra, C. Y. Ang and J. Y. Ying, *Angew. Chem., Int. Ed.*, 2007, **46**, 2448–2452.
- R. Bakalova, Z. Zhelev, I. Aoki, K. Masamoto, M. Mileva, T. Ohba, M. Higuchi, V. Gadjeva and I. Kanno, *Bioconjugate Chem.*, 2008, **19**, 1135–1142.